JOURNAL OF GEOPHYSICAL RESEARCH, VOL. 99, NO. D9, PAGES 18,973–18,987, SEPTEMBER 20, 1994

Seasonal variability of vertical eddy diffusivity in the middle atmosphere
1. Three-year observations by the middle and upper atmosphere radar

Shoichiro Fukao,[1] Manabu D. Yamanaka,[1] Naoki Ao,[1,2] Wayne K. Hocking,[3] Toru Sato,[4] Mamoru Yamamoto,[1] Takuji Nakamura,[1] Toshitaka Tsuda,[1] and Susumu Kato[1,5]

Abstract. The vertical eddy diffusivity K due to atmospheric turbulence with spatial scales of 10^0–10^2 m has been computed from the echo power spectral width observed by the middle and upper atmosphere radar for almost every month from January 1986 to December 1988. The method of analysis follows *Lilly et al.* [1974], *Sato and Woodman* [1982], and *Hocking* [1983a, 1985, 1988], and the contamination due to beam broadening, vertical shear, and transience has been removed. Although observations for horizontal wind speeds larger than approximately 40 m/s, such as occur near the tropopause jet stream in winter, have been omitted because of excessive beam broadening, sufficient numbers of observations have been accumulated to produce a reasonable climatology for the upper troposphere and lower stratosphere (6–20 km altitude) and for the mesosphere (60–82 km altitude). The monthly median of K shows a local maximum near the tropopause jet stream altitude. It becomes larger in the mesosphere, increasing gradually with height. Maxima of K are observed in winter near the tropopause and in summer in the mesosphere, and the seasonal variability of K reaches approximately an order of magnitude. A semiannual variability is apparent in the mesosphere with minima in the equinoctial seasons.

1. Introduction

The vertical eddy diffusivity K is one of the most important parameters needed to model the transport of minor constituents such as ozone in the middle atmosphere. However, since direct measurements of turbulence have not been easy for a long time except by sophisticated rocket [*Teitelbaum and Blamont*, 1977; *Thrane et al.*, 1985; *Lübken et al.*, 1987], balloon [*Barat*, 1975, 1982; *Yamanaka et al.*, 1985; *Dalaudier and Sidi*, 1987], and aircraft [*Lilly et al.*, 1974] observations, K has been inferred largely from the vertical distribution of atmospheric constituents, usually ignoring the effects of seasonal and meridional variations [*Johnson and Wilkins*, 1965; *Justus*, 1973; *McElroy et al.*, 1974; *Shimazaki and Ogawa*, 1974; *Crutzen*, 1974; *Johnston et al.*, 1976; *Ogawa and Shimazaki*, 1975; *Blum and Schuchardt*, 1978; *Massie and Hunten*, 1981; *Allen et al.*, 1981; *Strobel et al.*, 1987]. Such an ad hoc description has also been used in dynamical models of gravity-wave dissipation [*Matsuno*, 1982]. Chemically deduced values of K are often affected by the lifetime of each constituent and include not only the true diffusion effect due to microscale turbulence but also an advection effect due to the meridional circulation [*Strobel*, 1989; *McIntyre*, 1989] and/or planetary waves [cf. *Matsuno*, 1980; *Holton*, 1981]. Since *Lindzen* [1981] proposed his well-known parameterization scheme for K due to purely monochromatic internal gravity waves, modelers have incorporated it into their models [e.g., *Holton*, 1982; *Garcia and Solomon*, 1985].

Recently, mesosphere-stratosphere-troposphere (MST) and mesosphere/lower-thermosphere (MLT) radars have provided a powerful measurement technique for determination of K over a quite broad altitude range, with far better temporal resolution than previously afforded with the other techniques. There are two main procedures which may be used to infer K. Firstly, we may estimate characteristics of the target scattering the radio wave from the radar echo power intensity [*Gage et al.*, 1980; *Balsley and Garello*, 1985; *Sato et al.*, 1985]. We then use relationships between the refractive index gradient and the turbulence parameters [e.g., *Tatarski*, 1971] to infer K, but the accuracy of this method decreases when temperature and humidity are not known with high resolution. Alternatively, we can extract the mean kinetic energy dissipation rate ε from the echo power spectral width, which is dependent directly upon the variance of wind velocity fluctuations inside the radar scattering volume. The observed value of ε can then be converted into an estimate for K under reasonable assumptions [*Lilly et al.*, 1974]. This technique was first applied systematically by *Sato and Woodman* [1982] to the tropical lower

[1]Radio Atmospheric Science Center, Kyoto University, Uji, Kyoto, Japan.
[2]Now at Matsushita Electric Works, Limited, Kadoma, Osaka, Japan.
[3]Department of Physics, University of Western Ontario, London, Canada.
[4]Department of Electrical Engineering II, Kyoto University, Sakyo, Kyoto.
[5]Professor Emeritus of Kyoto University.

Paper number 94JD00911.
0148-0227/94/94JD-00911$05.00

stratosphere, and it was developed comprehensively by *Hocking* [1983a, b, 1986].

In the uppermost part of the middle atmosphere, radar observations provide fairly reliable estimates of K, which are necessary to determine the homopause (or turbopause) level at an altitude in the region 100–120 km [*Hocking*, 1985, 1987, 1988, 1989, 1990, 1991]. However, in the 60- to 100-km altitude range, recent in situ measurements sometimes show smaller values of K than those used in many one-dimensional chemical models [*Thrane et al.*, 1985; *Lübken et al.*, 1987], and some chemical model studies also require smaller values of K [*Allen et al.*, 1981; *Strobel et al.*, 1987]. Small-scale inhomogeneities of middle atmospheric turbulence, generated possibly by gravity-wave breaking, have been actually observed with in situ measurements [*Lilly et al.*, 1974; *Barat*, 1975, 1982; *Yamanaka et al.*, 1985; *Cot and Barat*, 1986; *Thrane et al.*, 1987] as well as with MST radars [*Sato and Woodman*, 1982; *Woodman and Rastogi*, 1984; *Sato et al.*, 1985; *Yamamoto et al.*, 1987]. All of these observations except for those in the mesopause region done by *Hocking* [1988] over 2 years were case studies, and the seasonal variability of K is not well known and quite controversial. For example, in the mesopause region the photochemical model of *Blum and Schuchardt* [1978] and the dynamical-chemical model of *Garcia and Solomon* [1985] suggested a maximum of K in the summer at middle to high latitudes, whereas semitheoretical estimations by *Ebel* [1980] and *Danilov and Kalgin* [1992] concluded that there is a maximum of K in the winter hemisphere, and the seasonal variability in *Hocking*'s [1988, 1989] observations is very weak in comparison with smaller-scale and interannual variations. Therefore a climatological description throughout the middle atmosphere, from which we may exactly estimate a net transport due to true turbulent diffusion processes, has yet to be presented.

The purpose of this two-part study is to establish a climatology of K in the middle atmosphere, based on long-term observations with an MST radar technique and on gravity-wave breaking theory. In part 1 we show seasonal variations of K due to atmospheric turbulence computed from the echo power spectral width observed every month during 1986–1988 by the middle and upper atmosphere (MU) radar in Japan (35°N, 136°E). It must be noted that our observations are limited to locally homogeneous turbulence with spatial scales $\leq 10^2$ m and that different values of K may apply to highly inhomogeneous atmospheric motions with different (larger) spatial scales [e.g., *Dewan*, 1981]. The MU radar experiments and data reduction procedures used to obtain K are described in section 2, together with a description of our procedure for removal of contamination (mainly due to background wind). In sections 3 and 4 we show observational results of the seasonal variability of K for the tropostratosphere and the mesosphere, respectively. Finally, we summarize the observational results in section 5. Details of an interpretation in view of gravity-wave breaking theory will be described in part 2 (M. D. Yamanaka and S. Fukao, Seasonal variability of vertical eddy diffusivity in the middle atmosphere, 2, Gravity wave breaking theory and parameterization, submitted to *Journal of Geophysical Research*, 1994].

2. Observational Principle

2.1. Middle and Upper Atmosphere (MU) Radar

The MU radar is a VHF-band (46.5 MHz) Doppler radar which has an active phased-array system composed of 475 Yagi antennas with nominal peak and average transmitted powers of 1 MW and 50 kW, respectively, and a receiver dynamic range of 70 dB [*Fukao et al.*, 1985a, b, 1990]. It observes atmospheric echoes from the altitude ranges of 1–25 km (day and night) and 55–90 km (daytime only). This radar can be steered to any position within 30° of zenith each interpulse period (400 μs minimum), which enables us to observe in five directions in only 2 ms, for example. Beside applying these and other capabilities of the MU radar to various scientific objectives, we have been carrying out a standard program of observation continuously for about 100 hours every month, which was initiated in 1985 as campaign-based work under the gravity waves and turbulence in middle atmosphere cooperation (GRATMAC) program. The present study is based on the data set of GRATMAC observations for 1986–1988, as listed in Table 1. The parameters used in the GRATMAC observations are listed in Table 2, and details are described by *Fukao et al.* [1991].

The MU radar detects Doppler velocity spectra associated with eddies of spatial scales ranging from half the radar wavelength (3 m) up to the sampled volume thickness (in this study 150 m for the troposphere and stratosphere and 600 m

TABLE 1. List of the GRATMAC Standard Observations

Case	Year/Date/LST
Jan. 1986	1986/Jan. 6/1109 to Jan. 10/1303
Feb. 1986	1986/Feb. 10/1304 to Feb. 14/1547
March 1986	1986/March 17/0800 to March 21/1542
April 1986	1986/April 7/1134 to April 11/1528
May 1986	1986/May 6/1123 to May 9/1535
June 1986	1986/June 2/1200 to June 6/1426
July 1986	1986/July 7/1156 to July 11/1329
Aug. 1986	1986/Aug. 18/1017 to Aug. 22/1416
Sept. 1986	1986/Sept. 1/1201 to Sept. 5/1639
Oct. 1986	1986/Oct. 13/1120 to Oct. 17/1535
Nov. 1986	1986/Nov. 10/2357 to Nov. 14/1536
Jan. 1987	1987/Jan. 5/1316 to Jan. 9/1530
Feb. 1987	1987/Feb. 3/0053 to Feb. 6/1529
March 1987	1987/March 2/1201 to March 6/1536
April 1987	1987/April 6/1104 to April 10/1536
May 1987	1987/May 11/1344 to May 15/1536
June 1987	1987/June 22/1200 to June 26/1200
July 1987	1987/July 6/1723 to July 11/0544
Aug. 1987	1987/Aug. 3/1217 to Aug. 7/1220
Sept. 1987	1987/Sept. 7/1151 to Sept. 11/1634
Oct. 1987	1987/Oct. 5/1207 to Oct. 9/1454
Nov. 1987	1987/Oct. 26/1135 to Oct. 30/1505
Dec. 1987	1987/Dec. 7/1037 to Dec. 11/1517
Jan. 1988	1988/Jan. 5/0818 to Jan. 8/1434
Feb. 1988	1988/Feb. 15/1214 to Feb. 19/1517
March 1988	1988/March 7/0823 to March 11/1537
April 1988	1988/April 18/0915 to April 22/1530
May 1988	1988/May 9/0847 to May 13/1521
June 1988	1988/June 6/1156 to June 10/1641
July 1988	1988/July 18/1559 to July 22/1637
Aug. 1988	1988/Aug. 8/1137 to Aug. 12/1628
Sept. 1988	1988/Aug. 29/1237 to Sept. 2/1532
Oct. 1988	1988/Oct. 24/1146 to Oct. 28/1527
Nov. 1988	1988/Nov. 14/1501 to Nov. 18/1527
Dec. 1988	1988/Dec. 19/0814 to Dec. 23/1600

GRATMAC, gravity waves and turbulence in middle atmosphere cooperation.

TABLE 2. Parameters of the MU Radar for the GRATMAC Standard Observations

	Troposphere/Stratosphere	Mesosphere
Observation period	all day	daytime (~0600–1800 LST)
Sampling interval	150 s	150 s
Altitude range	5.4–24.5 km	60–98 km
Altitude resolution	150 m	600 m (sampled every 300 m)
Beam directions (zenith, azimuth)	upward (0°, 0°), northward (10°, 0°), eastward (10°, 90°), southward (10°, 180°), and westward (10°, 270°)	upward (0°, 0°), northward (10°, 0°), eastward (10°, 90°), southward (10°, 180°), and westward (10°, 270°)
Signals		
interpulse period (IPP)	400 μs	730 μs
pulse compression	16-bit complementary	8-bit complementary
Data processing		
coherent integrations	38 times	20 times
incoherent integrations	6 times	6 times

MU, middle and upper atmosphere.

for the mesosphere). The MU radar therefore can provide turbulence characteristics for scale sizes that extend approximately over the entire inertial subrange of three-dimensional (locally isotropic and homogeneous) atmospheric turbulence, as shown in Figure 1. The largest scale of eddies observed with the MU radar is slightly smaller than the largest scale of the inertial subrange estimated from foregoing studies [e.g., *Hocking*, 1985, 1987]. The nominal beam ($1/e$) width is 3.6°, corresponding to horizontal diameters of <1 and ~4 km at altitudes of ~10 and ~70 km, respectively. We can convert the half-power half width $\sigma_{1/2}$ of the Doppler velocity spectrum to the variance of the radial (line of sight) velocity $\sqrt{\overline{(u_r')^2}}$ (u_r' is a deviation from the mean radial velocity) inside the sampled volume through the simple relationship

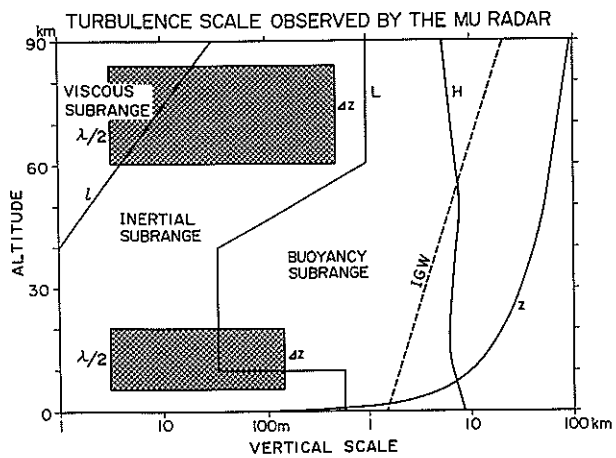

Figure 1. Vertical scales of the inertial subrange of turbulence (L, the outer scale; l, the inner scale), adapted from *Hocking* [1985] with modifications. Observable scales with the middle and upper atmosphere (MU) radar (Δz, the sampled volume thickness; $\lambda/2$, half the radar wavelength) are hatched. The density scale height (H), the predominant vertical wavelength (IGW, to be discussed in part 2), and the maximum vertical scale (Z, given by the altitude itself) are also indicated. Note that L and l correspond to k_B^{-1} and k_ν^{-1}, respectively, in the text.

$$\overline{(u_r')^2} = \frac{\sigma_{1/2}^2}{2 \ln 2} \approx 0.72\sigma_{1/2}^2, \tag{1}$$

as described by *Hocking* [1983a, 1985].

To extract turbulence parameters from $\sigma_{1/2}$, we postulate that we observe the entire inertial subrange obeying the Kolmogorov −5/3 power law for the power spectrum of the scalar wavenumber k. The following derivation is a variant on that produced by *Hocking* [1983a, 1986] and approximately follows *Sato and Woodman* [1982]. We may write [*Frisch and Clifford*, 1974; *Bohne*, 1982],

$$\frac{3}{2}\overline{(u_r')^2} \approx \int_{k_B}^{k_\nu} \alpha \varepsilon^{2/3} k^{-5/3}\, dk \tag{2}$$

where α (≈1.5) is the Kolmogorov constant, ε is the mean kinetic energy dissipation rate, $k_B \equiv N/\sqrt{\overline{(u_r')^2}}$ is the lowest wavenumber of the inertial subrange (the highest wavenumber of the buoyancy subrange), N is the Väisälä-Brunt frequency to be defined in (9), and k_ν is the highest wavenumber of the inertial subrange (the inverse dimension of the minimum eddy surviving in a viscous atmosphere). Performing the integration on the right-hand side of (2) and noting that ε is constant in the inertial subrange, we obtain

$$\varepsilon \approx CN\overline{(u_r')^2}, \qquad C = \alpha^{-3/2}\left[1 - \left(\frac{k_B}{k_\nu}\right)^{2/3}\right]^{-3/2}.$$

If $k_\nu \gg k_B$, then $C \approx \alpha^{-3/2} \approx 0.5$. In the present study, following *Weinstock* [1981a], who has shown that $C \approx 0.4$ for many observations, and using (1), we extract ε from $\sigma_{1/2}$ through

$$\varepsilon \approx 0.3N\sigma_{1/2}^2, \tag{3}$$

if N is known by an appropriate temperature observation. Prior to converting ε to K in section 3.3, we shall examine the observational errors of $\sigma_{1/2}$ in section 3.2.

2.2. Observational Limit due to Spectral Broadening Effects

When we allow for a finite beam width and a finite sampling duration, the radial velocities are not uniform in the

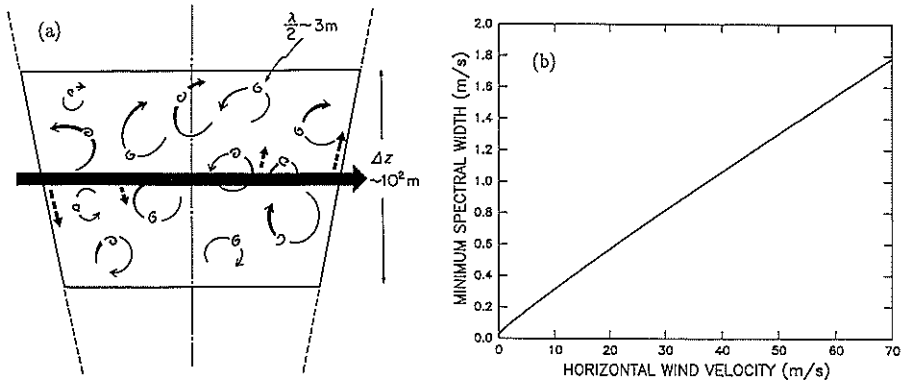

Figure 2. The observational principle and beam-broadening contamination due to a background wind. (a) Schematic vertical cross section of a radar scattering volume in which λ/2-scale eddies are advected by larger-scale turbulence; the background wind (thick horizontal arrow) produces an inhomogeneous radial velocity field which appears as beam broadening in the observed Doppler spectra. (b) Calculated relationship between the background horizontal wind velocity and the minimum spectral width observed by the MU radar (zenith angle, 10°).

sampled volume, so that the experimental value of spectral width, say, $\sigma_{1/2}$, obs, includes several components which are not directly produced by turbulence. *Atlas et al.* [1969], *Frisch and Clifford* [1974], and *Hocking* [1983a, 1985, 1986, 1988] showed that there are spectral broadening effects due to (1) horizontal winds, (2) wind shear, and/or (3) transience of atmospheric motions.

Effect 1, the so-called beam-broadening effect, arises because different radial Doppler velocities are observed in different parts (different line-of-sight directions) within a finite beam width (see Figure 2a). The contribution of this effect to the observed spectral width is

$$\sigma_{1/2\text{beam}} \approx \delta_{1/2}|\bar{\mathbf{u}}_h|, \tag{4}$$

where $\delta_{1/2}$ (≈1.3° ≈ 0.023 rad for the MU radar) is the half-power half width of the effective (two way) radar beam, and $\bar{u}_h$ is the background horizontal velocity [see also *Hocking et al.*, 1990]. This effect increases monotonically with increasing $\bar{u}_h$ and induces a serious error in strong wind conditions, as will be described below.

Effect 2, the shear broadening effect, arises when the radial component of the wind changes over the sampled volume. This effect is evaluated for horizontal shear as

$$\sigma_{1/2\text{shear}} \approx \frac{1}{2}\left|\frac{\partial \bar{\mathbf{u}}_h}{\partial z}\right|\Delta z \sin 10° \tag{5}$$

for a beam with a zenith angle of 10° and a sampled volume thickness Δz (equal to 150 m (troposphere and stratosphere) or 600 m (mesosphere) for the present observation with the MU radar). When the background atmospheric stratification is stable, that is, the background Richardson number is given by

$$\overline{Ri} \equiv \frac{N^2}{|\partial \bar{\mathbf{u}}_h/\partial z|^2} > \frac{1}{4},$$

we have $\sigma_{1/2\text{shear}} < N\Delta z \sin 10° \ll 1$ m/s. See *Hocking* [1983a] for more thorough numerical simulations of this effect.

Effect 3, contamination due to transience of atmospheric motions, arises when the wind changes during a length of time τ (≈73 s in the present case) used for incoherent integration. The variance of the radial velocity for the interval τ is given by *Hocking* [1988] as

$$\overline{(u'_\tau)^2} \approx \frac{W^2}{2}\left[1 - \frac{2}{N^2\tau^2}(1 - \cos N\tau)\right],$$

assuming that the variance is mainly due to Väisälä-Brunt oscillations with amplitude W. However, we cannot observe $\overline{(u'_\tau)^2}$ directly from observations, since, in general, W is not known. Instead, we specify the variance $\overline{(u'_{2\tau})^2}$ for 2τ, which may be similarly written by replacing τ by 2τ, from observations with an approximately Gaussian-distributed histogram of the difference between two sequential records of radial velocities. Therefore transience contamination can be estimated as

$$\begin{aligned}\sigma^2_{1/2\text{trans}} &= 2 \ln 2\overline{(u'_\tau)^2} \\ &\approx 2 \ln 2 \frac{1 - (2/N^2\tau^2)(1 - \cos N\tau)}{1 - (1/2N^2\tau^2)(1 - \cos 2N\tau)}\overline{(u'_{2\tau})^2} \\ &\approx 4\overline{(u'_{2\tau})^2}.\end{aligned} \tag{6}$$

The contaminations (effects 1–3) mentioned above are removed from the measured spectral width $\sigma_{1/2\text{obs}}$ to produce the spectral width due to turbulence alone $\sigma_{1/2}$ as

$$(\sigma_{1/2})^2 = (\sigma_{1/2\text{obs}})^2 - (\sigma_{1/2\text{beam}})^2 - (\sigma_{1/2\text{shear}})^2 - (\sigma_{1/2\text{trans}})^2. \tag{7}$$

For the usual MST radar observations with sufficiently small zenith angles, effect 1 is the most serious contamination, as is described below.

In the case of the MU radar observations the estimation error of the radial velocity becomes [*Yamamoto et al.*, 1988].

$$\Delta \approx 1.1\sqrt{\frac{\sigma_{1/2\text{obs}}}{\tau}}\ [\text{m/s}].$$

The estimation error of the spectral width is also approximately Δ. Therefore a necessary condition for obtaining $\sigma_{1/2}$ from observations of $\sigma_{1/2\text{obs}}$ by an oblique beam with a zenith angle of 10° is given by

$$(\sigma_{1/2\text{obs}} - \sqrt{2\ln 2}\Delta)^2 > \left(\sigma_{1/2\text{beam}} + \frac{\delta_{1/2}\Delta}{\sin 10°}\right)^2,$$

that is, from (4),

$$\sigma_{1/2\text{obs}} > \sigma_{1/2\text{min}} \equiv \left(\frac{A + \sqrt{A^2 + 4\delta_{1/2}|\bar{\mathbf{u}}_h|}}{2}\right)^2,$$

$$A \equiv \frac{1.1}{\sqrt{\tau}}\left(\sqrt{2\ln 2} + \frac{\delta_{1/2}}{\sin 10°}\right) \approx 0.155[(\text{m/s})^{1/2}].$$

The relationship between $\sigma_{1/2\text{min}}$ and $|\bar{\mathbf{u}}_h|$ is plotted in Figure 2b.

According to in situ measurements in the lower stratosphere, isotropic turbulence has a typical maximum root-mean-square fluctuating velocity of 1 m/s [*Barat*, 1975, 1982; *Yamanaka et al.*, 1985]. We find from Figure 2b that the Doppler spectral width due to beam broadening then exceeds 1 m/s when the horizontal wind speed exceeds 40 m/s. Therefore σ cannot be extracted from the spectral width in a horizontal wind speed ≥40 m/s. Such wind speeds appear frequently near the tropopause jet stream in winter, when the observed values of σ are close to semitheoretical calculations of the beam broadening, as shown in the top panels of Figure 3. However, as shown in the bottom panels of Figure 3 and also in Figure 4, observations during other seasons or at other altitudes are not correlated with the beam-broadening effects. These discussions follow closely *Hocking* [1985, 1986].

2.3. Estimation of Vertical Eddy Diffusivity

The vertical eddy diffusivity K is introduced by a parameterization of the vertical heat flux by using the vertical gradient of the mean potential temperature, that is,

$$K = -\overline{\theta' w'}\Big/\frac{\partial\bar{\theta}}{\partial z}, \tag{8}$$

where z is altitude, w is vertical velocity, θ is potential temperature, and the overbar and prime denote the mean field and perturbations, respectively.

The mean temperature field is parameterized in terms of N defined by

$$N^2 \equiv \frac{g}{\bar{\theta}}\frac{\partial\bar{\theta}}{\partial z} = \frac{g}{\bar{T}}\left(\frac{\partial\bar{T}}{\partial z} + \frac{g}{C_p}\right), \tag{9}$$

where T is temperature, g is gravitational acceleration, and C_p is specific heat at constant pressure. It must be noted that N is a slowly varying parameter of the mean field, so that we do not need very high resolution for the temperature data to determine N. We consider a condition of thermal equilibrium, with energy generation due to the Reynolds stress and energy dissipation due to turbulence, such that

$$\varepsilon = -\frac{\partial\bar{u}}{\partial z}\overline{u'w'} + \frac{g}{\bar{\theta}}\overline{\theta' w'} = \left(1 - \frac{1}{R_f}\right)\frac{g}{\bar{\theta}}\overline{\theta' w'},$$

where u is the horizontal velocity and

$$R_f \equiv \frac{g}{\bar{\theta}}\overline{\theta' w'}\Big/\frac{\partial\bar{u}}{\partial z}\overline{u'w'},$$

is the flux Richardson number.

Substituting these expressions into (8), we have

$$K = \frac{\beta\varepsilon}{N^2} \text{ and } \beta \equiv \frac{R_f}{1 - R_f}. \tag{10}$$

It must be noted that (10) gives a local value of K for (locally) homogeneous turbulence (inside a layered or patchy region) and that different formulations of K may be more appropriate for different spatial and/or temporal scales (e.g., larger than those of layered structures). Although *Dewan* [1981] proposed another formula giving a bulk value for a larger region containing extremely inhomogeneous turbulence with thin intermittent layers, (10) is applicable for our observations with sufficiently good resolution to see inside such turbulence layers (see sections 2.1 and 2.4). The formula (10) is also derived under gravity-wave breaking theories [see *Weinstock*, 1984, 1990; *McIntyre*, 1989]. These points will be again discussed in part 2.

As an experimental evaluation of the nondimensional factor β in the lower stratosphere, *Lilly et al.* [1974] used $R_f = 1/4$ and obtained

$$\beta = \frac{1}{3} \approx 0.3, \tag{11}$$

while *Weinstock* [1978] proposed $\beta \approx 0.8$, based on a semitheoretical approach for turbulence spreading into adjoint stable regions ($R_f \approx 4/9$). Although some observational studies [*Thrane et al.*, 1985; *Lübken et al.*, 1987] used the latter evaluation, *Weinstock* [1981b] showed a generalized formula $\beta \approx 0.8/[1 + 0.6k_0^2\overline{(u')^2}/N^2] < 0.8$ for a dominant wavenumber k_0 in the turbulence energy spectrum. This formula gives $\beta \approx 0.8$ when very large eddies are dominant ($k_0 \ll k_B \equiv N/\sqrt{\overline{(u_r')^2}} \sim 2\pi/O(10^2\ \text{m})$), but $\beta \approx 1/3$ when the dominant turbulence scale is slightly smaller than the buoyancy scale ($k_0 \approx 1.5k_B$). *Hocking* [1987] summarized that β lies between 0.2 and 1 and suggested that $\beta \approx 1$ is suitable only if the homopause level is fixed at around 110 km altitude. A recent paper by *von Zahn et al.* [1990] (also see *Weinstock* [1984, 1990]), applying an approximation used by *Tatarski* [1971], uses another formula $\beta \approx Ri$ (the local Richardson number) ≈1/4, which agrees roughly with $\beta \approx 0.3$. In part 2 we will show that $\beta \approx 0.3$ is not too far from the results of observations on the localization of turbulence due to breaking gravity-wave structure.

Substituting (11) and (3) into (10), we finally obtain

$$K \approx 0.1\frac{\sigma_{1/2}^2}{N}. \tag{12}$$

This is the basic formula used in part 1 of this study.

2.4. Method of Calculation

The following procedure was followed in our determination of K. First of all, we omitted unreliable records by

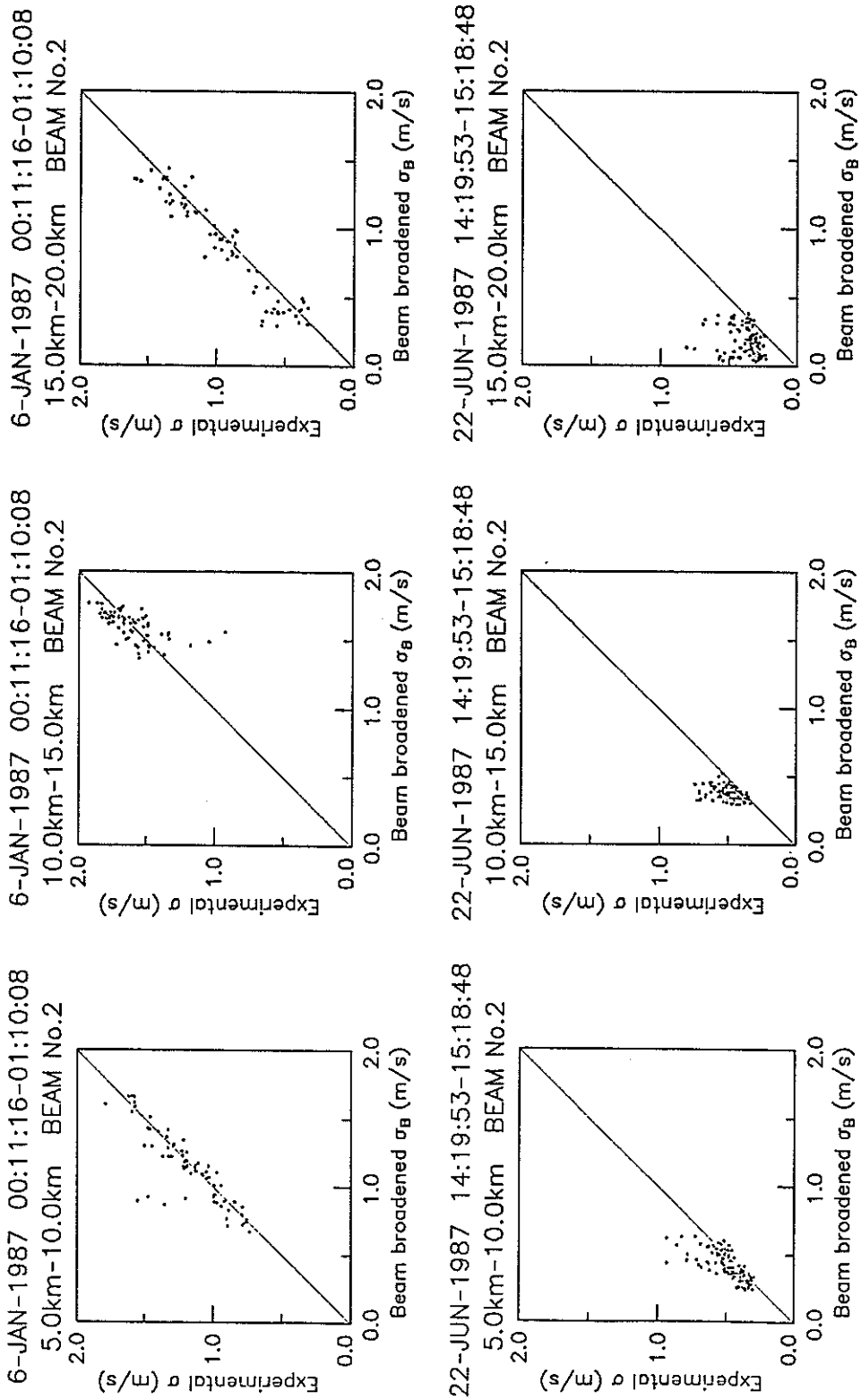

Figure 3. Scatter plots of experimental spectral half-power half width of oblique beams at 10° azimuth versus the beam-broadening contaminations for the upper troposphere and lower stratosphere. The three top panels show the winter case, and the three bottom panels show the summer case.

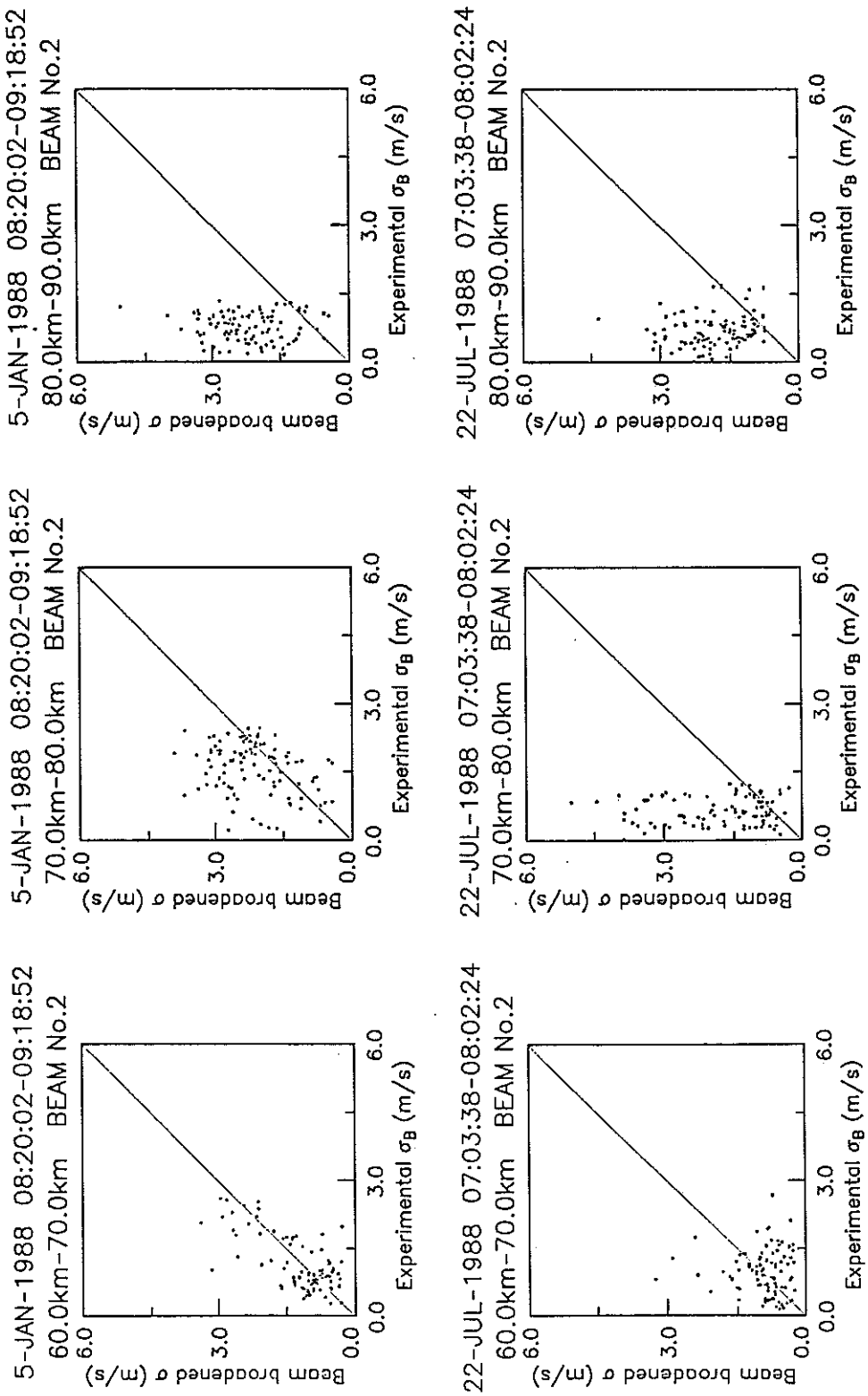

Figure 4. Same as Figure 3 but for the mesosphere.

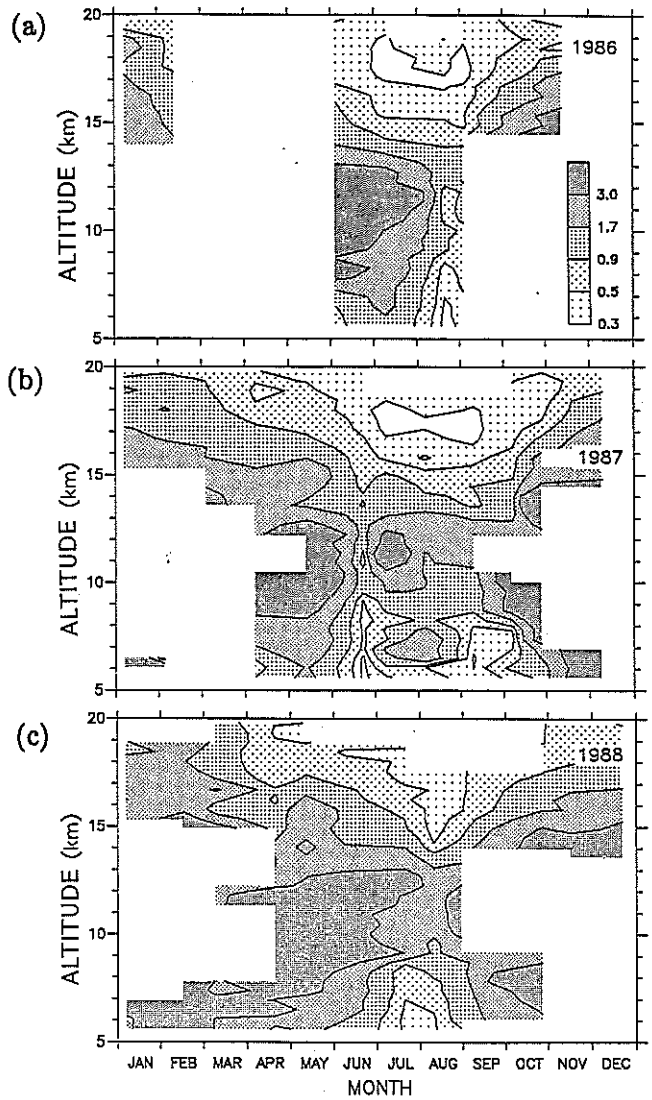

Figure 5. Seasonal-vertical variations of the monthly medians of vertical eddy diffusivity K observed by the MU radar in the upper troposphere and lower stratosphere in (a) 1986, (b) 1987, and (c) 1988, respectively. Units are in m^2/s.

applying a median filter of echo power, Doppler frequency, and spectral width as functions of time and altitude and averaged the data for 30 min in the tropostratosphere and for 1 hour in time and 1.2 km in altitude in the mesosphere. It must be noted that resolutions are still better than the outer scales (thickness or lifetime) of turbulence structures in the middle atmosphere, even after those averaging procedures. Following this, we calculated $\sigma_{1/2\text{obs}}$ for each of the four oblique beams listed in Table 2, and $\overline{u_h}$ from all the five beams. Next, we obtained $\sigma_{1/2\text{beam}}$ and $\sigma_{1/2\text{shear}}$ for each oblique beam from $\overline{u_h}$ and $|\partial\overline{u_h}/\partial z|$ through (4) and (5), respectively. Third, $\sigma_{1/2\text{trans}}$ was specified by making a histogram of 1000 samples of the temporal difference of radial velocity from the original data (without averaging) inside an altitude range of 1 km in the tropostratosphere and in the entire observed range in the mesosphere for each oblique beam every month, by using (6). Fourth, $\sigma_{1/2}$ was obtained by averaging the values calculated by using (7) for each oblique beam. Last, for each altitude we took a median of the K values extracted from $\sigma_{1/2}$ through (12) each month.

In this paper (part 1 of the two-part study), N in the stratosphere and troposphere was interpolated from values calculated by using 12 hourly routine rawinsonde data obtained at Hamamatsu Station (34°N, 137°E, about 150 km east of the MU radar) of the Japan Defense Agency and published monthly as *Aerological Data of Japan* by the Japan Meteorological Agency (JMA). N in the mesosphere was calculated as a function of month and altitude by using the first draft of the CIRA(1986) data sets published by *Barnett and Corney* [1985].

The first attempt to extract turbulence parameters from the MU radar observations with a similar technique was done by *Sato et al.* [1986]. In this preliminary stage the authors used the vertical beam for omitting data affected by background shear and considered that the results were not completely reliable mainly because sufficient height resolution in N could not be obtained. However, the value of N may be assumed to be slowly varying in comparison to the velocity variations, as was mentioned before. Nevertheless, an analysis similar to that portrayed in Figure 3 for the vertical beam has shown that we often cannot extract $\sigma_{1/2}$ for the vertical beam, because this beam is affected by partial reflection rather than by isotropic scattering due to isotropic turbulence. Therefore we used the oblique beams and relatively rough temperature profiles. We have successfully accumulated data over 3 years for the upper troposphere, lower stratosphere, and mesosphere and have obtained reasonable results, as will be demonstrated in sections 3 and 4.

3. Upper Troposphere and Lower Stratosphere

Figure 5 shows seasonal-vertical variations of the monthly medians of K obtained from the GRATMAC observations by the MU radar during 1986–1988 in the upper troposphere and lower stratosphere. We observe from this result that K takes its maximum value near the tropopause jet stream in winter and the seasonal variability reaches about an order of magnitude, although observations near the tropopause jet stream in winter are less reliable, as mentioned in section 2.2. The height of this maximum seems to be reasonable, since the mean vertical shear maximizes and hence the mean dynamic stability minimizes near the tropopause jet stream in winter, which has been confirmed by the MU radar and by 12 hourly routine rawinsonde observations at JMA stations. To support this further, we show in Figure 6 the seasonal-vertical variations of ε calculated approximately by [*Tatarski*, 1971],

$$\varepsilon \approx \gamma \left| \frac{\partial \bar{u}_h}{\partial z} \right|^3 L^2 \tag{13}$$

where we put $\gamma = 1$ and $L = 10$ m after *VanZandt et al.* [1981], and the vertical shear $|\partial\bar{u}_h/\partial z|$ is obtained from routine observations in 1985 at Shionomisaki Station (33°N, 136°E, about 150 km south of the MU radar) of JMA. This result supports the maximum activity of turbulence near the tropopause jet stream in winter and the seasonal variability reaching an order of magnitude, although ε given by (13) is somewhat smaller than that calculated by (3) because the scale L might be variable and slightly underestimated. (We

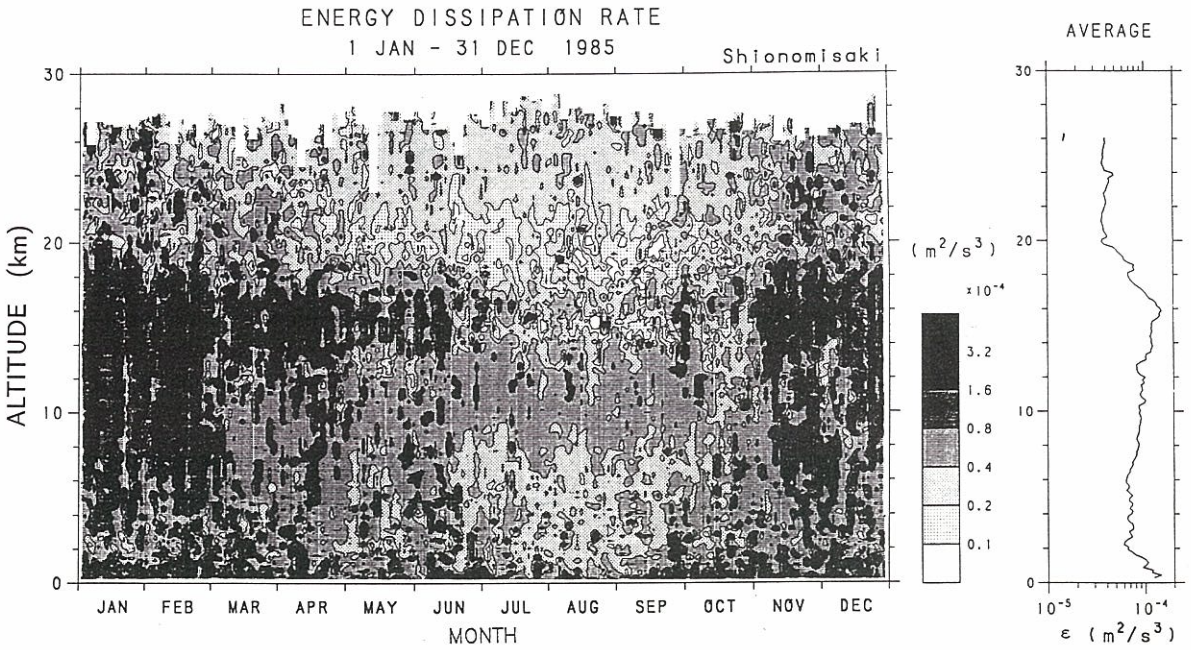

Figure 6. Seasonal-vertical variations of the mean kinetic energy dissipation rate ε calculated from routine meteorological observations (twice a day) at the Shionomisaki Weather Station of the Japan Meteorological Agency.

have estimated the variability of L by comparing the observational and theoretical values of the refractivity turbulence structure constant $C_n^2 = 2.8M^2L^{4/3}$, where M is the gradient of generalized potential refractive index [*Tatarski*, 1971; *VanZandt et al.*, 1981] given as a function of pressure, temperature, and humidity. About 66% of the estimated values of L are between 8 and 13 m, so that $L = 10$ m is considered to be in a good approximation. The variance of L (about 20%) cannot explain the seasonal variability of ε (or K), which is much larger than 40%.)

Figures 7 and 8 show the vertical profiles of the annual and seasonal medians of K, respectively, during 1986–1988 in the upper troposphere and lower stratosphere, compared with a standard model profile [*Massie and Hunten*, 1981]. The magnitude of K in the lower stratosphere is quite close to (in summer) or slightly larger than (in winter) that estimated from modeling studies, which implies that the vertical transport process in the lower stratosphere is mainly due to turbulent mixing inside thin intermittent layers. Such layered turbulence frequently appears in the lower stratosphere, especially in winter above the strong tropopausal jet stream and is quite different from the patchy turbulence observed in the troposphere [e.g., *Fukao et al.*, 1986]. In the troposphere, layered turbulence appears predominantly near frontal surfaces extending continuously to the tropopause. This difference between the troposphere and the stratosphere also provides an objective means for determining the tropopause level and frontal surface by radar techniques [*Gage and Green*, 1979; *Rastogi and Röttger*, 1982; *Larsen and Röttger*, 1985; *Gage et al.*, 1986; *Larsen et al.*, 1991]. These inhomogeneities may lead to a variability of K over a vertical scale ≤ 1 km and a timescale ≤ 1 day, but this small-scale variability is smoothed out when we take a median for ~100 hours each month, since turbulence layers and patches can be considered to appear with equal probability over the whole altitude range observed during a time interval ≥ 1 day.

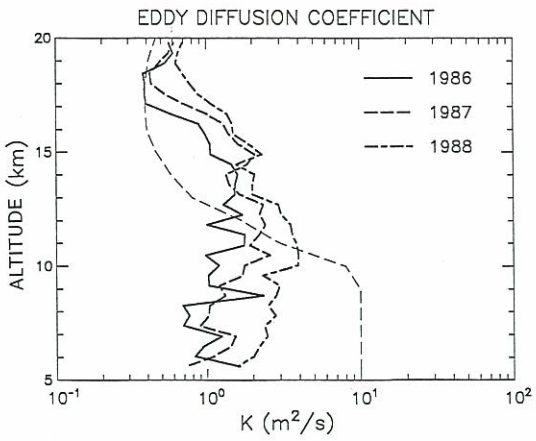

Figure 7. Vertical profiles of the annual medians of vertical eddy diffusivity K observed by the MU radar during 1986–1988 in the upper troposphere and lower stratosphere, in comparison with a standard model profile [*Massie and Hunten*, 1981].

The winter maximum of K and the sporadic nature of turbulence layers in the lower stratosphere may explain the large differences in values of K deduced from the foregoing studies, as mentioned in section 1. First, the differences between case studies are reasonable because turbulence appears sporadically both in time and in altitude and its activity varies with season. Those features are characteristic of turbulence generated by breaking of internal gravity waves [e.g., *Geller et al.*, 1975; *Fritts and Rastogi*, 1985], and a winter maximum has been found also for gravity wave activity in the lower stratosphere [*Murayama et al.*, 1994; *Sato*, 1994]. Second, since the time and spatial scales of

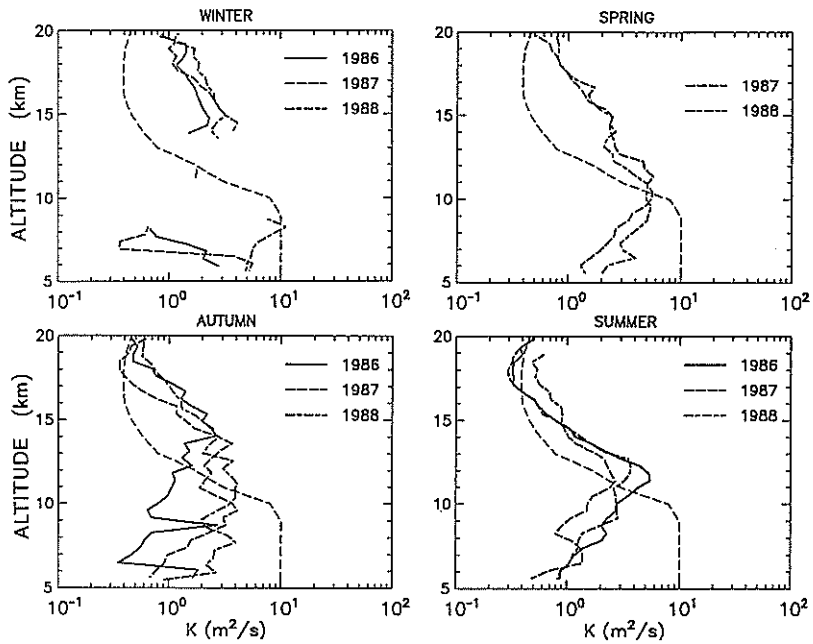

Figure 8. Vertical profiles of the seasonal medians of vertical eddy diffusivity K observed by the MU radar during 1986–1988 in the upper troposphere and lower stratosphere, in comparison with a standard model profile [*Massie and Hunten*, 1981].

eddies may be dependent upon those of the predominant internal gravity waves (as will be discussed in part 2), the diffusion effect on chemical constituents should vary with their lifetimes and distributions. Typical values of the time, horizontal and vertical scales of the predominant gravity waves in the lower stratosphere are $\sim O$(6 hours), $\sim O$(200 km), and $\sim O$(2 km), respectively [e.g., *Yamanaka*, 1991]. Broadly distributed long-life constituents such as ozone and carbon dioxide are governed by K with values similar to the present observations [*Shimazaki and Ogawa*, 1974; *Johnston et al.*, 1976], but short-life constituents such as nitrogen dioxide may be affected by somewhat different values of K induced by smaller eddies.

On the other hand, the magnitude of K in the troposphere in every season is smaller than the values presumed in the one-dimensional chemical models, except for a narrow altitude range during winter. It is considered by modelers that advection and diffusion due to synoptic- and/or planetary-scale waves may be more important causes of mixing in the troposphere and stratosphere than eddy diffusion [*Matsuno*, 1980; *Holton*, 1981]. Such a large-scale quasi-horizontal mixing is considered to take place along isentropes, so that this effect becomes quite large in the troposphere, whereas it is not so strong in the stratosphere where the isentropes are almost horizontal. A recent estimation of K due to the large-scale mixing (excluding the zonal mean advection effect) based on a general circulation model [*Yamazaki*, 1989] shows a maximum of 3–4 m^2/s near the frontal zones in the midlatitude middle troposphere, another maximum of 2–3 m^2/s in the equatorial middle troposphere, and a minimum less than 1 m^2/s in the midlatitude lower stratosphere, which implies that the magnitude and vertical/seasonal variabilities of K due to large-scale mixing are quite similar to those of K due to the microscale turbulence observed here. This similarity is reasonable, if we notice the fact that synoptic-scale waves produce multiple tropopause levels and frontal surfaces through the cyclogenesis mechanism and consider that these "multiple tropopauses" are nothing more than the multiple turbulence layers observed in the troposphere and stratosphere [see *Yamanaka*, 1991].

4. Mesosphere

Figure 9 shows the seasonal-vertical variations of monthly medians of K for the mesosphere. Figures 10 and 11 show vertical profiles of annual and seasonal medians of K, respectively, in comparison with a standard model profile [*Ogawa and Shimazaki*, 1975]. We clearly find from these figures that K becomes larger in the mesosphere than in the tropostratosphere and increases gradually with height, as shown in case studies and models made so far. The magnitude of K is smaller than that required to simulate chemical transport [*Ogawa and Shimazaki*, 1975] and wave dissipation [*Matsuno*, 1982] properly in one-dimensional models, although chemical models for short lifetime species [*Crutzen*, 1974; *Allen et al.*, 1981; *Strobel et al.*, 1987] and recent rocket measurements in northern Europe [*Thrane et al.*, 1985, 1987; *Lübken et al.*, 1987, 1993; *von Zahn et al.*, 1990] often suggest magnitudes of K smaller than the aforementioned models. The distributions of the hourly medians and profiles of the range, including 66% of the data, are also plotted in Figures 10 and 11. From this we conclude that the magnitude of K observed by the MU radar is seldom close to the value predicted by the models for species with long lifetimes. The smaller-scale variability or inhomogeneity of K, which induces a diffusion effect dependent upon the chemical lifetime and distribution scale (see paragraph 3 of section 3), is due to the characteristics of the origin of the turbulence, i.e., breaking gravity waves.

Layered turbulence also frequently appears in the mesos-

phere, but its thickness is several times larger than that in the lower stratosphere [*Yamamoto et al.*, 1987]. Such thick turbulence layers are generated by breaking gravity waves with intrinsic periods of around 10 hours and vertical wavelengths longer than the order of 1 km [*Tsuda et al.*, 1990a; *Murayama et al.*, 1992] and possibly include eddies with dimensions of the order of 1 km. Those large eddies may induce a large value of K, as will be discussed in part 2, which cannot be extracted with the present experimental technique because the sampling volume is too small. (We might obtain K due to such a large eddy by summing two or three adjacent range values, but the contamination discussed in section 2 becomes larger by this summation.) Similar observations with an MF-band (2 MHz) radar employing coarser resolution (2 km) than the present study have shown much larger values of K in the mesopause region above 80 km [*Hocking*, 1983, 1988], in spite of the recent rocket measurements showing smaller values even in altitude regions similar to (or somewhat higher than) those of our observations [*Thrane et al.*, 1985, 1987; *Lübken et al.*, 1987, 1993; *von Zahn et al.*, 1990]. Because the latter measurements have finer vertical resolution (~10 m), we can hardly consider that our low values of K result from the coarser resolution of our radar measurements. The low reliability of N also may induce an underestimation of K by using (12), as noted in section 2.4. Additionally, advective transport due to the mean meridional circulation, rather than the eddy diffusion, should be taken into account in model studies of the atmospheric constituents [*McIntyre*, 1989; *Strobel*, 1989; *Danilov and Kalgin*, 1992]. Recent work by *Walterscheid and Hocking* [1991] has suggested that Stokes drift due to a random collection of gravity waves may also contribute to large-scale diffusion.

The seasonal maximum of K in the mesosphere is observed in summer, which is strikingly different from the case in the tropostratosphere, and the seasonal variability reaches an order of magnitude. It is interesting that gravity-wave activity (and the resultant momentum flux and energy den-

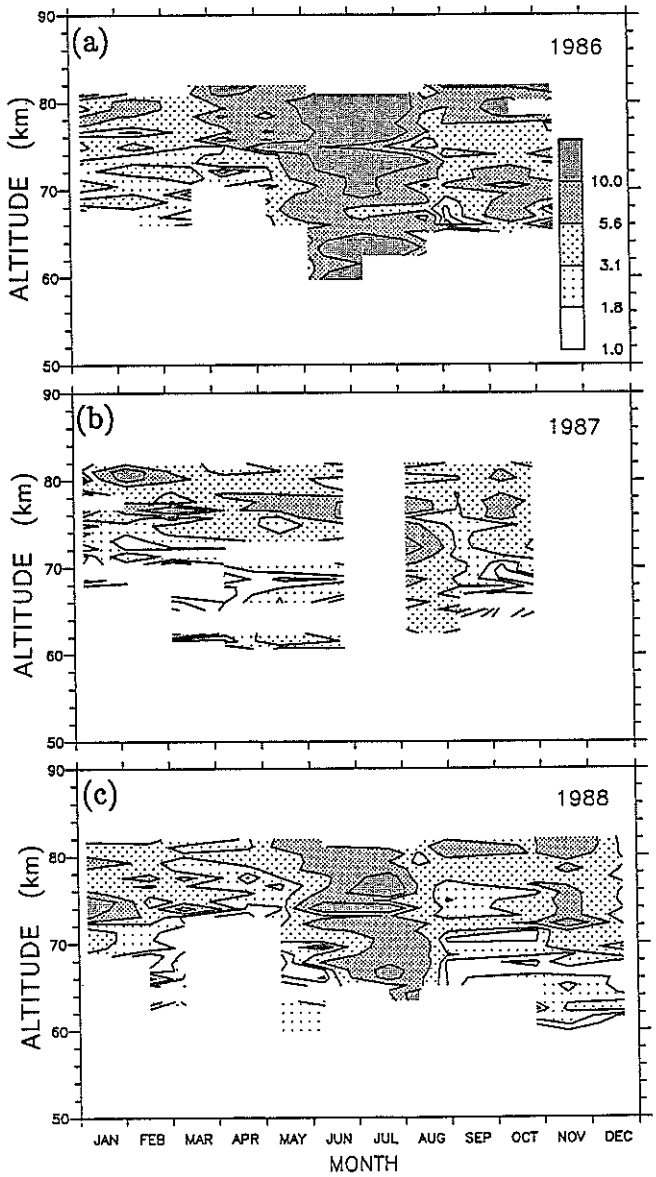

Figure 9. Same as Figure 5 but for the mesosphere.

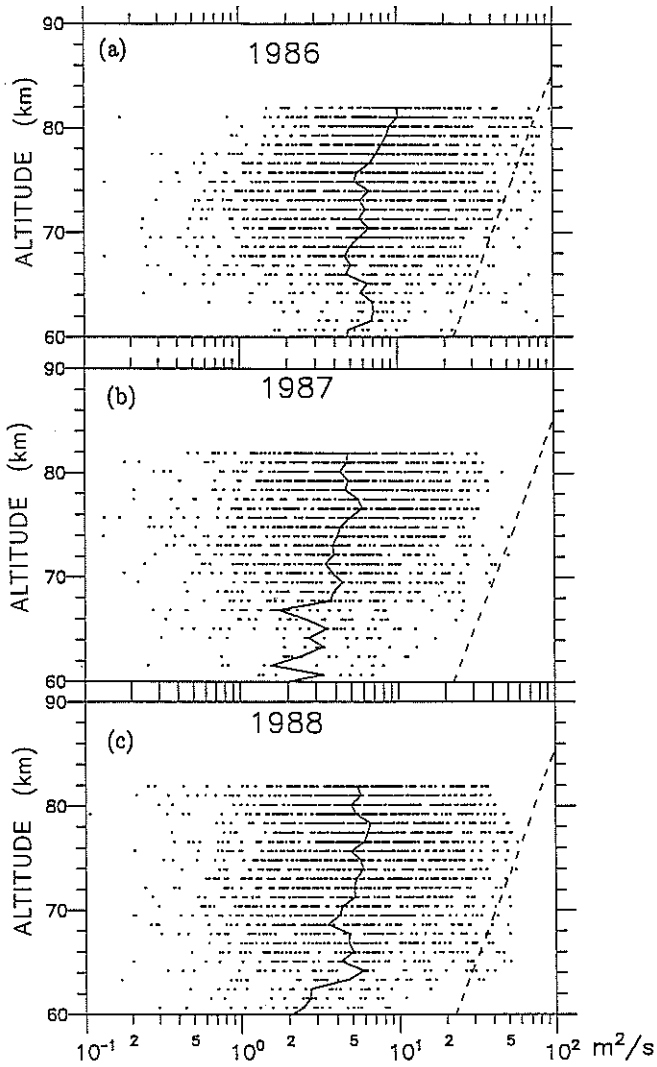

Figure 10. Scatter plots of the hourly medians and the vertical profiles of annual medians of vertical eddy diffusivity K observed by the MU radar in the mesosphere for (a) 1986, (b) 1987, and (c) 1988, in comparison with a standard model profile [*Ogawa and Shimazaki*, 1975].

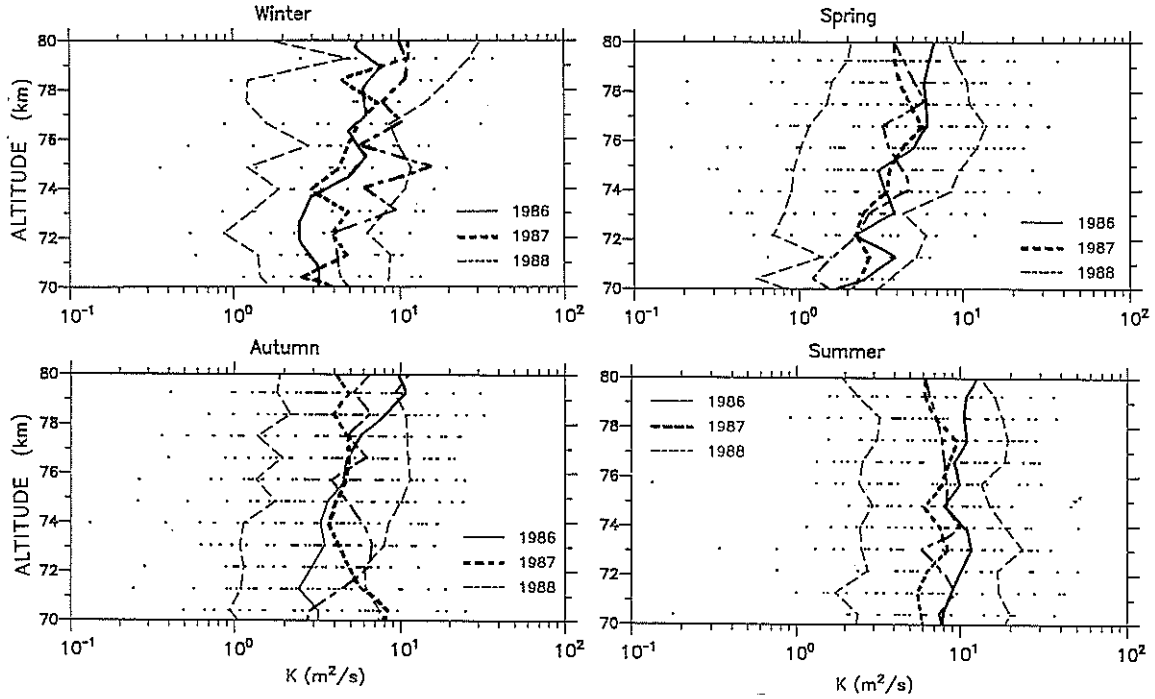

Figure 11. Vertical profiles of the seasonal medians of vertical eddy diffusivity K observed by the MU radar in the mesosphere during 1986–1988. Hourly median values for each season in 1987 are plotted by dots, 66% of which are ranged between a pair of thick broken curves.

sity) observed by the MU radar or by lidars in the mesosphere also shows a maximum in summer [*Tsuda et al.*, 1990b, 1994; *Wilson et al.*, 1991]. If gravity waves are most active in summer, it is reasonable that K due to wave breaking turbulence becomes largest in summer. A weak semiannual variability of K is also found in our observations, as noted by *Hocking* [1988]. The summer maximum and weak semiannual variability in the mesosphere are consistent with the results of the chemical-dynamical coupling model of *Garcia and Solomon* [1985], who incorporated gravity-wave breaking. These results support the hypothesis that middle-atmospheric turbulence is mainly induced by breaking of internal gravity waves, which will be discussed in detail in part 2 of this study. The seasonal variability mentioned above is also consistent with estimations of K in the homopause (or turbopause) region by *Blum and Schuchardt* [1978], and this fact suggests that the homopause level is controlled by gravity-wave breaking.

On the other hand, our results are not consistent with the winter maximum of K suggested by *Ebel* [1980] and *Danilov and Kalgin* [1992]. This is reasonable because Ebel considered all the dynamical effects including advection due to meridional circulation and planetary-scale disturbances; the latter effects are much stronger in winter than in summer, at least in the mesosphere [e.g., *Hitchman et al.*, 1989]. Although Danilov and Kalgin considered that the mean upward (downward) advection in summer (winter) could contribute to an "apparent" summer maximum of K for "upward decreasing" constituents in the lower thermosphere, such a situation may not always hold in the mesosphere.

Furthermore, although *Hocking* [1988] reported a large interannual variation of K in the mesopause region observed with the Adelaide MF radar during 1985–1986 (see also *Hocking* [1989] for 1987 data), we do not find any systematic difference among the three years (1986–1988) analyzed monthly (Figure 10). Since Hocking analyzed 1-week averages, the seasonal variability may not appear predominant in comparison with large-amplitude smaller-scale variations. To confirm whether our results are universal or not, we need to make observations in various geographical locations.

The MU radar observations are only possible during daytime in the mesosphere, and one may wonder if K changes at night. Tidal variations become predominant in the mesosphere, particularly in the upper mesosphere, and many physical quantities there are known to vary with local time. However, the typical vertical wavelengths of internal gravity waves observed by lidars at night in similar altitude regions [*Chanin and Hauchecorne*, 1981; *Wilson et al.*, 1991] are not different from those observed by the MU radar in the daytime [*Murayama et al.*, 1992; *Tsuda et al.*, 1994]. MF radars can be used for mesopause region observations both in daytime and in nighttime, but they also do not detect strong diurnal variations of the typical vertical wavelength [*Manson and Meek*, 1988; *Vincent*, 1990]. Therefore as long as middle-atmospheric turbulence is generated mainly by gravity-wave breaking, the values of K in the nighttime should be similar to those in the daytime. (In fact, *Hocking* [1988] found no systematic diurnal variations in turbulence parameters from his MF radar observations, although he did not explicitly discuss this fact in his paper.)

5. Summary and Discussions

Table 3 shows a summary of the MU radar observations of K described in this paper. First of all, K is larger in the mesosphere than in the stratosphere for every season. It is

one of our important findings that in the lower stratosphere the contribution to K from 10^0 to 10^2 m scale eddies inside layered structures, which are possibly induced by gravity-wave breaking, has the magnitude required by modeling studies for the appropriate transport of minor atmospheric constituents. In the troposphere and also in the mesosphere, on the other hand, the contribution to K from turbulence induced by breaking gravity waves with a vertical wavelength of few kilometers seems smaller than the values required by many models for appropriate chemical transport and wave dissipation, and the effects of advective motions and larger-scale diffusion are more important. These features are again emphasized in Figure 12, which summarizes a comparison between the MU radar observations and the previous studies cited in section 1. In part 2 of this study, the upward increasing character of K will be explained based on the fact that the predominant vertical wavelength of gravity waves increases with altitude. Large differences among various observations and models for the mesosphere and lower thermosphere, as shown in Figure 12, may be due to both localized/sporadic wave breaking and chemical lifetime.

Secondly, maxima of K are observed in winter near the tropopause and in summer in the mesosphere. These seasonal variabilities of K, reaching approximately an order of magnitude, are likely to be directly related to those of breaking gravity waves. The power and momentum flux of gravity waves observed by the MU radar in the mesosphere also have maxima in summer, whereas the source of gravity waves near the tropopause may be more active in winter than the other seasons [*Tsuda et al.*, 1990b, 1994; *Wilson et al.*, 1991; *Murayama et al.*, 1994; *Sato*, 1994]. We can easily confirm that the mean vertical shear over the MU radar also has a summer maximum in the mesosphere and a winter maximum near the tropopause. In part 2 we will show that the seasonal variability of K induced by breaking of the predominant modes of internal gravity waves is related to the magnitude of the mean vertical shear, if the breaking wavelength is approximately given by a function only of altitude.

Finally, based on the present results, we can consider that the parameterization scheme of K described in section 2 is valid at least for turbulence induced by gravity-wave breaking. More specifically, K derived by using (12) is the isotropic diffusion constant for heat inside a thin turbulence layer induced by gravity-wave breaking. The atmosphere is no doubt anisotropic for larger-scale motions, and the large-scale diffusion constants for heat, momentum, and mass are different from K obtained in this paper [e.g., *Dewan*, 1981; *McIntyre*, 1989; *Strobel*, 1989]. This fact suggests a limitation in applying the conventional K parameterization to transport problems, but the idea of K parameterization itself is valid for a limited type of dynamical phenomenon of the atmosphere. We need much more data on the variability of turbulence and gravity wave parameters, including those which seem constant to a first-order approximation.

TABLE 3. Summary of Observations

	Troposphere/Stratosphere	Mesosphere
Magnitude	$\sim 10^0$ m^2/s	$\sim 10^1$ m^2/s
Maximum altitude	~10 km	increasing upward
Maximum season	winter	summer
Dominant mode	annual	semiannual

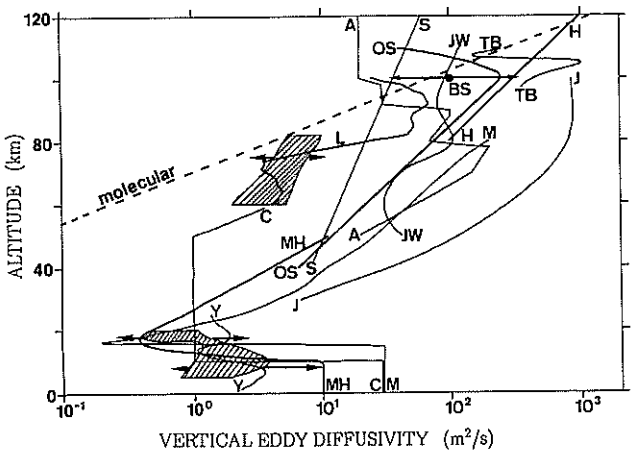

Figure 12. Comparison of the present observations (the variability of the annual medians is shown by the hatched areas) with previous studies (*A* [*Allen et al.*, 1981]; *BS* [*Blum and Schuchardt*, 1978]; *C* [*Crutzen*, 1974]; *H* [*Hocking*, 1985b]; *J* [*Justus*, 1973]; *JW* [*Johnson and Wilkins*, 1965]; *L* [*Lübken et al.*, 1993]; *M* [*McElroy et al.*, 1974]; *MH* [*Massie and Hunten*, 1981]; *OS* [*Ogawa and Shimazaki*, 1975]; *TB* [*Teitelbaum and Blamont*, 1977]; *S* [*Strobel et al.*, 1987]; and *Y* [*Yamazaki*, 1989]). The seasonal variabilities obtained by the present observations (as the ranges of the seasonal medians) and by the study of Blum and Schuchardt are shown by arrows. An approximate profile of the molecular diffusivity is also indicated by broken curve.

Acknowledgments. The JMA data for making Figure 6 were provided by Isamu Hirota of Kyoto University. Thanks are also due to William L. Oliver of Boston University for his careful reading of the manuscript. The authors were partly supported by grants in aid (02NP0201, 03NP0201 and 05NP0201) of the Ministry of Education, Science and Culture of Japan. The MU radar belongs to and is operated by the Radio Atmospheric Science Center, Kyoto University.

References

Allen, M., Y. L. Yung, and J. W. Waters, Vertical transport and photochemistry in the terrestrial mesosphere and lower thermosphere (50–120 km), *J. Geophys. Res.*, *86*, 3617–3627, 1981.

Atlas, D., R. C. Srevastava, and P. W. Sloss, Wind shear and reflectivity gradient effects on Doppler radar spectra, II, *J. Appl. Meteorol.*, *8*, 384–388, 1969.

Balsley, B. B., and R. Garello, The kinetic energy density in the troposphere, stratosphere and mesosphere: A preliminary study using the Poker Flat MST radar in Alaska, *Radio Sci.*, *20*, 1355–1361, 1985.

Barat, J., Etude expérimentale de la structure du champ de turbulence dans la moyenne stratosphère, *C. R. Acad. Sci.*, *B280*, 691–693, 1975.

Barat, J., Some characteristics of clear air turbulence in the middle stratosphere, *J. Atmos. Sci.*, *39*, 2553–2564, 1982.

Barnett, J. J., and M. Corney, Middle atmosphere reference model derived from satellite data, *Handb. MAP*, *16*, 86–137, 1985.

Blum, P. W., and K. G. H. Schuchardt, Semi-theoretical global models of the eddy diffusion coefficient based on satellite data, *J. Atmos. Terr. Phys.*, *40*, 1137–1142, 1978.

Bohne, A. R., Radar detection of turbulence in precipitation environments, *J. Atmos. Sci.*, *39*, 1819–1837, 1982.

Chanin, M.-L., and A. Hauchecorne, Lidar studies of gravity and

tidal waves in the stratosphere and mesosphere, *J. Geophys. Res.*, *86*, 9715–9721, 1981.
Cot, C., and J. Barat, Wave-turbulence interaction in the stratosphere: A case study, *J. Geophys. Res.*, *91*, 2749–2756, 1986.
Crutzen, P., A review of upper atmospheric photochemistry, *Can. J. Chem.*, *52*, 1569–1581, 1974.
Dalaudier, F., and C. Sidi, Evidence and interpretation of a spectral gap in the turbulent atmospheric temperature spectra, *J. Atmos. Sci.*, *44*, 3121–3126, 1987.
Danilov, A. D., and U. A. Kalgin, Seasonal and latitudinal variations of eddy diffusion coefficient in the mesosphere and lower thermosphere, *J. Atmos. Terr. Phys.*, *54*, 1481–1489, 1992.
Dewan, E. M., Turbulent vertical transport due to thin intermittent mixing layers in the stratosphere and other stable fluids, *Science*, *211*, 1041–1042, 1981.
Ebel, A., Eddy diffusion models for the mesosphere and lower thermosphere, *J. Atmos. Terr. Phys.*, *42*, 617–628, 1980.
Frisch, A. S., and S. F. Clifford, A study of convection capped by a stable layer using Doppler radar and acoustic echo sounders, *J. Atmos. Sci.*, *31*, 1622–1628, 1974.
Fritts, D. C., and P. K. Rastogi, Convective and dynamical instabilities due to gravity wave motions in the lower and middle atmosphere: Theory and observations, *Radio Sci.*, *20*, 1247–1277, 1985.
Fukao, S., T. Sato, T. Tsuda, S. Kato, K. Wakasugi, and T. Makihira, The MU radar with an active phased array system, 1, Antenna and power amplifiers, *Radio Sci.*, *20*, 1155–1168, 1985a.
Fukao, S., T. Tsuda, T. Sato, S. Kato, K. Wakasugi, and T. Makihira, The MU radar with an active phased array system, 2, In-house equipment, *Radio Sci.*, *20*, 1169–1176, 1985b.
Fukao, S., T. Sato, T. Tsuda, M. Yamamoto, and S. Kato, High resolution turbulence observations in the middle and lower atmosphere by the MU radar with fast beam steerability: Preliminary results, *J. Atmos. Terr. Phys.*, *48*, 1269–1278, 1986.
Fukao, S., T. Sato, T. Tsuda, M. Yamamoto, M. D. Yamanaka, and S. Kato, MU radar: New capabilities and system calibrations, *Radio Sci.*, *25*, 477–485, 1990.
Fukao, S., M. F. Larsen, M. D. Yamanaka, H. Furukawa, T. Tsuda, and S. Kato, Observations of a reversal in long-term average vertical velocities near the jet stream wind maximum, *Mon. Weather Rev.*, *119*, 1479–1489, 1991.
Gage, K. S., and J. L. Green, Tropopause detection by partial specular reflection using VHF radar, *Science*, *203*, 1238–1240, 1979.
Gage, K. S., J. L. Green, and T. E. VanZandt, Use of Doppler radar for the measurement of atmospheric turbulence parameters from the intensity of clear air echoes, *Radio Sci.*, *15*, 407–416, 1980.
Gage, K. S., W. L. Ecklund, A. C. Riddle, and B. B. Balsley, Objective tropopause height determination using low-resolution VHF radar observations, *J. Atmos. Oceanic Technol.*, *3*, 248–254, 1986.
Garcia, R. R., and S. Solomon, The effect of breaking gravity waves on the dynamics and chemical composition of the mesosphere and lower thermosphere, *J. Geophys. Res.*, *90*, 3850–3868, 1985.
Geller, M. A., H. Tanaka, and D. C. Fritts, Production of turbulence in the vicinity of critical levels for internal gravity waves, *J. Atmos. Sci.*, *32*, 2125–2135, 1975.
Hitchman, M. H., J. C. Gille, C. D. Rodgers, and G. Brasseur, The separated polar winter stratopause: A gravity wave driven climatological feature, *J. Atmos. Sci.*, *46*, 410–422, 1989.
Hocking, W. K., On the extraction of atmospheric turbulence parameters from radar backscatter Doppler spectra, I, Theory, *J. Atmos. Terr. Phys.*, *45*, 89–102, 1983a.
Hocking, W. K., Mesospheric turbulence intensities measured with a HF radar at 35°S, II, *J. Atmos. Terr. Phys.*, *45*, 103–114, 1983b.
Hocking, W. K., Measurements of turbulent energy dissipation rate in the middle atmosphere by radar techniques: A review, *Radio Sci.*, *20*, 1403–1422, 1985.
Hocking, W. K., Observation and measurements of turbulence in the middle atmosphere with a VHF radar, *J. Atmos. Terr. Phys.*, *48*, 655–670, 1986.
Hocking, W. K., Turbulence in the region 80–120 km, *Adv. Space Res.*, *7*(10), 171–181, 1987.
Hocking, W. K., Two years of continuous measurements of turbulence parameters in the upper mesosphere and lower thermosphere made with a 2-MHz radar, *J. Geophys. Res.*, *93*, 2475–2491, 1988.
Hocking, W. K., Seasonal variation of turbulence intensities in the upper mesosphere and lower thermosphere measured by radar techniques during the 3-year period 1985–1987, *Handb. MAP*, *28*, 309–310, 1989.
Hocking, W. K., Turbulence in the region 80–120 km, *Adv. Space Res.*, *10*(12), 153–161, 1990.
Hocking, W. K., The effects of middle atmosphere turbulence on coupling between atmospheric regions, *J. Geomagn. Geoelectr.*, *43*, 621–636, 1991.
Hocking, W. K., S. Fukao, T. Tsuda, M. Yamamoto, T. Sato, and S. Kato, Aspect sensitivity of stratospheric VHF radio wave scatterers, particularly above 15-km altitude, *Radio Sci.*, *25*, 613–627, 1990.
Holton, J. R., An advective model for two-dimensional transport of stratospheric trace species, *J. Geophys. Res.*, *86*, 11,989–11,994, 1981.
Holton, J. R., The role of gravity wave induced drag and diffusion in the momentum budget of the mesosphere, *J. Atmos. Sci.*, *39*, 791–799, 1982.
Johnson, F. S., and E. M. Wilkins, Thermal upper limit on eddy diffusion in the mesosphere and lower thermosphere, *J. Geophys. Res.*, *70*, 1281–1284, 1965.
Johnston, H. S., D. Kattenhorn, and G. Whitten, Use of excess carbon 14 data to calibrate models of stratospheric ozone depletion by supersonic transports, *J. Geophys. Res.*, *81*, 368–380, 1976.
Justus, C. G., Upper atmospheric mixing by gravity waves, *AIAA/AMS Pap. 73-495*, June 11–13, 1973.
Larsen, M. F., and J. Röttger, Observations of frontal zone and tropopause structures with a VHF Doppler radar and radiosondes, *Radio Sci.*, *20*, 1223–1232, 1985.
Larsen, M. F., S. Fukao, O. Aruga, M. D. Yamanaka, T. Tsuda, and S. Kato, A comparison of VHF radar vertical measurements by a direct vertical beam method and by a VAD technique, *J. Atmos. Oceanic Technol.*, *8*, 766–776, 1991.
Lilly, D. K., D. E. Waco, and S.-I. Adelfang, Stratospheric mixing estimated from high-altitude turbulence measurements, *J. Appl. Meteorol.*, *13*, 488–493, 1974.
Lindzen, R. S., Turbulence and stress owing to gravity wave and tidal breakdown, *J. Geophys. Res.*, *86*, 9707–9714, 1981.
Lübken, F.-J., U. von Zahn, E. V. Thrane, T. A. Blix, G. A. Kokin, and S. V. Pachomov, In situ measurements of turbulence energy dissipation rates and eddy diffusion coefficients during MAP/WINE, *J. Atmos. Terr. Phys.*, *49*, 763–775, 1987.
Lübken, F.-J., W. Hillert, G. Lehmacher, and U. von Zahn, Experiments revealing small impact of turbulence on the energy budget of the mesosphere and lower thermosphere, *J. Geophys. Res.*, *98*, 20,369–20,384, 1993.
Manson, A. H., and C. E. Meek, Gravity wave propagation characteristics (60–120 km) as determined by the Saskatoon MF radar (GRAVNET) system: 1983–85 at 52°N, 107°W, *J. Atmos. Sci.*, *45*, 932–946, 1988.
Massie, S. T., and D. M. Hunten, Stratospheric eddy diffusion coefficients from tracer data, *J. Geophys. Res.*, *86*, 9859–9868, 1981.
Matsuno, T., Lagrangian motion of air parcels in the stratosphere in the presence of planetary waves, *Pure Appl. Geophys.*, *118*, 189–216, 1980.
Matsuno, T., A quasi-one-dimensional model of the middle atmosphere circulation interacting with internal gravity waves, *J. Meteorol. Soc. Jpn.*, *60*, 215–226, 1982.
McElroy, M. B., S. C. Wofsy, J. E. Penner, and J. C. McConnell, Atmospheric ozone: Possible impact of stratospheric aviation, *J. Atmos. Sci.*, *31*, 287–300, 1974.
McIntyre, M. E., On the dynamics and transport near the polar mesopause in summer, *J. Geophys. Res.*, *94*, 14,617–14,628, 1989.
Murayama, Y., T. Tsuda, M. Yamamoto, T. Nakamura, T. Sato, S. Kato, and S. Fukao, Dominant vertical scales of gravity waves in the middle atmosphere observed with the MU radar and rocketsondes, *J. Atmos. Terr. Phys.*, *54*, 339–346, 1992.
Murayama, Y., T. Tsuda, and S. Fukao, Seasonal variation of gravity wave activity in the lower atmosphere, *J. Geophys. Res.*, in press, 1994.
Ogawa, T., and T. Shimazaki, Diurnal variations of odd nitrogen

and ionic densities in the mesosphere and lower thermosphere: Simultaneous solution of photochemical-diffusive equations, *J. Geophys. Res.*, *80*, 3945–3960, 1975.

Rastogi, P. K., and J. Röttger, VHF radar observations of coherent reflections in the vicinity of the tropopause, *J. Atmos. Terr. Phys.*, *44*, 461–469, 1982.

Sato, K., A statistical study on structure, saturation and sources of inertio-gravity waves in the lower stratosphere observed with the MU radar, *J. Atmos. Terr. Phys.*, in press, 1994.

Sato, T., and R. F. Woodman, Fine altitude resolution observations of stratospheric turbulent layers by the Arecibo 430-MHz radar, *J. Atmos. Sci.*, *39*, 2546–2552, 1982.

Sato, T., T. Tsuda, S. Kato, S. Morimoto, S. Fukao, and I. Kimura, High-resolution MST observations of turbulence using the MU radar, *Radio Sci.*, *20*, 1452–1460, 1985.

Sato, T., H. Matsumoto, S. Fukao, and S. Kato, Tropospheric turbulence parameters measured by using the MU radar, *Handb. MAP*, *20*, 99–102, 1986.

Shimazaki, T., and T. Ogawa, A theoretical model of minor constituent distributions in the stratosphere including diurnal variations, *J. Geophys. Res.*, *79*, 3411–3423, 1974.

Strobel, D. F., Constraints on gravity wave induced diffusion in the middle atmosphere, *Pure Appl. Geophys.*, *130*, 533–546, 1989.

Strobel, D. F., M. E. Summers, R. M. Bevilacqua, M. T. DeLand, and M. Allen, Vertical constituent transport in the mesosphere, *J. Geophys. Res.*, *92*, 6691–6698, 1987.

Tatarski, V. I., *The Effects of the Turbulent Atmosphere on Wave Propagation*, 472 pp., Keter Press, Jerusalem, 1971.

Teitelbaum, H., and J. Blamont, Variations of the turbopause altitude during the night, *Planet. Space Sci.*, *25*, 723–734, 1977.

Thrane, E. V., Ø. Andreassen, T. A. Blix, B. Grandal, A. Brekke, C. R. Philbrick, F. J. Schmidtlin, H.-U. Widdel, U. von Zahn, and F.-J. Lübken, Neutral air turbulence in the upper atmosphere observed during the energy budget campaign, *J. Atmos. Terr. Phys.*, *47*, 243–264, 1985.

Thrane, E. V., T. A. Blix, C. Hall, T. L. Hansen, U. von Zahn, W. Meyer, P. Czechowsky, G. Schmidt, H.-U. Widdel, and A. Neumann, Small scale structure and turbulence in the mesosphere and lower thermosphere at high latitudes in winter, *J. Atmos. Terr. Phys.*, *49*, 751–762, 1987.

Tsuda, T., S. Kato, T. Yokoi, T. Inoue, M. Yamamoto, T. E. VanZandt, S. Fukao, and T. Sato, Gravity waves in the mesosphere observed with the middle and upper atmosphere radar, *Radio Sci.*, *26*, 1005–1018, 1990a.

Tsuda, T., Y. Murayama, M. Yamamoto, S. Kato, and S. Fukao, Seasonal variation of momentum flux in the mesosphere observed with the MU radar, *Geophys. Res. Lett.*, *17*, 725–728, 1990b.

Tsuda, T., Y. Murayama, T. Nakamura, R. A. Vincent, A. H. Manson, C. E. Meek, and R. Wilson, Variations of the gravity wave characteristics with height, season and latitude revealed by comparative observations, *J. Atmos. Terr. Phys.*, *56*, 555–568, 1994.

VanZandt, T. E., K. S. Gage, and J. M. Warnock, An improved model for the calculation of profiles of C_n^2 and ε in the free atmosphere from background profiles of wind, temperature and humidity (reprints) in *20th Conference on Radar Meteorology*, pp. 129–135, American Meteorological Society, Boston, Mass., 1981.

Vincent, R. A., Planetary and gravity waves in the mesosphere and lower thermosphere, *Adv. Space Res.*, *10*(12), 93–97, 1990.

von Zahn, U., F.-J. Lübken, and C. Pütz, BUGATTI experiments: Mass spectrometric studies of lower thermosphere eddy mixing and turbulence, *J. Geophys. Res.*, *95*, 7443–7465, 1990.

Walterscheid, R. L., and W. K. Hocking, Stokes diffusion by atmospheric internal gravity waves, *J. Atmos. Sci.*, *48*, 2213–2230, 1991.

Weinstock, J., Vertical turbulent diffusion in a stably stratified fluid, *J. Atmos. Sci.*, *35*, 1022–1027, 1978.

Weinstock, J., Energy dissipation rates of turbulence in the stable free atmosphere, *J. Atmos. Sci.*, *38*, 880–883, 1981a.

Weinstock, J., Vertical turbulence diffusivity for weak or strong stable stratification, *J. Geophys. Res.*, *85*, 9925–9928, 1981b.

Weinstock, J., Gravity wave saturation and eddy diffusion in the middle atmosphere, *J. Atmos. Terr. Phys.*, *46*, 1069–1082, 1984.

Weinstock, J., Saturated and unsaturated spectra of gravity waves and scale-dependent diffusion, *J. Atmos. Sci.*, *47*, 2211–2225, 1990.

Wilson, R., M. L. Chanin, and A. Hauchecorne, Gravity waves in the middle atmosphere observed by Rayleigh lidar, II, Climatology, *J. Geophys. Res.*, *95*, 5169–5183, 1991.

Woodman, R. F., and P. K. Rastogi, Evaluation of effective eddy diffusive coefficients using radar observations of turbulence in the stratosphere, *Geophys. Res. Lett.*, *11*, 243–246, 1984.

Yamamoto, M., T. Tsuda, S. Kato, T. Sato, and S. Fukao, A saturated inertia gravity wave in the mesosphere observed by the middle and upper atmosphere radar, *J. Geophys. Res.*, *92*, 11,993–11,999, 1987.

Yamamoto, M., T. Sato, P. T. May, T. Tsuda, S. Fukao, and S. Kato, Estimation error of spectral parameters of mesosphere-stratosphere-troposphere radars obtained by least squares fitting method and its lower bound, *Radio Sci.*, *23*, 1013–1021, 1988.

Yamanaka, M. D., Formation of multiple tropopause and stratospheric inertio-gravity waves, *Adv. Space Res.*, *12*(10), 181–190, 1991.

Yamanaka, M. D., H. Tanaka, H. Hirosawa, Y. Matsuzaka, T. Yamagami, and J. Nishimura, Measurement of stratospheric turbulence by balloon-borne "glow-discharge" anemometer, *J. Meteorol. Soc. Jpn.*, *63*, 483–489, 1985.

Yamazaki, K., Diffusion coefficients derived from the Lagrangian statistics, *Proc. NIPR Symp. Polar Meteorol. Glaciol.*, *2*, 16–24, 1989.

N. Ao, Matsushita Electric Works, Ltd., Kadoma, Osaka 571, Japan.

S. Fukao, S. Kato, T. Nakamura, T. Tsuda, M. Yamamoto, and M. D. Yamanaka, Radio Atmospheric Science Center, Kyoto University, Uji, Kyoto 611, Japan.

W. K. Hocking, Department of Physics, University of Western Ontario, Loudon, Ontario NGA 3K7, Canada.

T. Sato, Department of Electrical Engineering II, Kyoto University, Sakyo, Kyoto 606, Japan.

(Received September 24, 1993; revised April 1, 1994;
accepted April 1, 1994.)